HHS Public Access

Author manuscript

Mol Cancer Ther. Author manuscript; available in PMC 2016 December 01.

Published in final edited form as:

Mol Cancer Ther. 2015 December ; 14(12): 2789–2796. doi:10.1158/1535-7163.MCT-15-0532.

Recombinant Immunotoxin with T Cell Epitope Mutations that Greatly Reduce Immunogenicity for Treatment of Mesothelin Expressing Tumors

Ronit Mazor, **Jingli Zhang**[1], **Laiman Xiang**, **Selamawit Addissie**, **Prince Awuah**, **Richard Beers**, **Raffit Hassan**[1], and **Ira Pastan**

Laboratory of Molecular Biology, Center for Cancer Research, National Cancer Institute, National Institutes of Health, Bethesda, MD

Abstract

SS1P is a recombinant immunotoxin (RIT) that targets mesothelin. It consists of an anti-mesothelin Fv fused to a portion of *Pseudomonas* exotoxin A. In clinical studies it has produced dramatic responses in patients with advanced mesothelioma, when combined with immunosuppressive therapy so that several treatment cycles could be given. Otherwise its activity is limited by its immunogenicity. In this work we describe the development and characterization of LMB-T20, a highly potent RIT targeted at mesothelin expressing cancers with low immunogenicity due to removal of its 8 T cell epitopes. LMB-T20 was more active than SS1P when tested on 4 different mesothelin expressing cell lines as well as on cells obtained from patients with mesothelioma. It also has potent anti-tumor activity in mice, and has reduced immunogenicity as measured by cytokine secretion assays. In conclusion, LMB-T20 is favorable candidate for evaluation in clinical trials due to its reduced immunogenicity and excellent activity.

Keywords

Immunotoxin; immunogenicity; mesothelin; T cell epitopes; deimmunization

Introduction

Recombinant immunotoxins (RITs) are genetically engineered chimeric proteins that are designed to treat cancer. RITs contain an antibody fragment that targets a cancer cell and a protein toxin that kills the cell. We have been developing immunotoxins that utilize a 38-Kda fragment of *Pseudomonas* exotoxin A (PE38) as a payload. When combined with agents that suppress the immune system or when used in patients whose immune systems are suppressed by the cancer, they have produced complete or near complete tumor regressions and prolonged life in patients with mesothelioma, hairy cell leukemia and acute

Corresponding author: Ira Pastan, Laboratory of Molecular Biology, NCI, 37 Convent Dr, Rm 5106, Bethesda, MD 20892.

[1]**Present address**: Thoracic and GI Oncology Branch, Center for Cancer Research, National Cancer Institute, National Institutes of Health, Bethesda, MD

Conflict of Interest: A patent has been filed by Ronit Mazor, Richard Beers and Ira Pastan for the investigational product in this research. Any patent awarded will be the property of the NIH. All authors declare no potential conflict of interest.

lymphoblastic leukemia (1, 2). An alternative approach is to diminish immunogenicity and improve efficacy by using protein engineering to make immunotoxins that are less immunogenic.

SS1P is a RIT that targets mesothelin. Mesothelin is a cell surface glycoprotein that is highly expressed on many malignancies including mesothelioma and cancers of the ovary, pancreas, lung, stomach and cervix (3–6). Because mesothelin is not expressed on essential normal organs, it is an attractive candidate for the therapy of solid tumors (7, 8). When SS1P was evaluated in clinical trials, it had low anti-tumor activity as a single agent and in most patients could only be given for a single cycle of three doses before neutralizing antibodies developed (8). However when it was combined with cytoxan and pentostatin to lower B and T cells and suppress anti-drug antibodies, more cycles could be given and major tumor responses were observed in patients with advanced refractory mesothelioma (9). These findings suggested that producing less immunogenic immunotoxins would be of great clinical value.

Immunogenicity often referred to as the formation of anti-drug antibodies (ADA) can cause adverse side effects (10) and have a dramatic effect on the potency and efficacy of protein therapeutics (11, 12). Immunogenicity is a general problem for protein based therapeutics and even human proteins can induce antibody formation, although they are much more common against non-human proteins. The antibodies involved in the immunogenicity response against SS1P are mostly high affinity IgGs reacting with PE38, the toxin portion of the RIT (13).

Elimination of T cell epitopes is beginning to be a well-accepted strategy to deimmunize protein therapeutics. Yeung *et al*. showed that elimination of a T cell epitope in the protein interferon beta (IFNβ) resulted in elimination of ADA response in BALB/c mice (14). We have previously reported the position of the human T-cell epitopes in the PE38 portion of immunotoxins targeting CD22 (15) and were able to decrease the T cell response to those epitopes by 90% in an *in vitro* system by introducing several point mutations and deleting a portion of domain II. This mutant RIT had a significant diminish in binding to serum from immunized patients (15).

The goal of this study was to design and evaluate the cytotoxic and anti-tumor activity and the immunogenicity of a new RIT that reacts with mesothelin expressing cancer cells, because patients could benefit greatly from treatment with such an agent.

Materials and Methods

Construction, expression and purification of RIT

SS1P, SS1P-LR-GGS and LMB-T20 are composed of the heavy-chain Fv fused to PE38 or PE24 toxin, with a disulfide-linkage to the light-chain Fv (V_L). For LMB-T20 plasmid design, the plasmids for SS1P (16) were used for the heavy-chain Fv (V_H) and V_L and the plasmid for LMB-T18 (15) was used for the T cell deimmunized toxin moity. The DNA encoding LMB-T20 was sequenced and expressed in *E. coli* as inclusion bodies. The RITs

were purified by a standard protocol (17). All RITs used in this study were >95% pure as assessed by SDS gel electrophoresis.

Cytotoxicity Assays

Cytotoxic activity in established mesothelin expressing cell lines—Cell responses to varying concentrations of RIT were evaluated on mesothelin expressing lines (A431/H9, KLM1, L55, MKN74, and HAY) using a WST8 cell-counting kit (Dojindo Molecular Technologies) according to manufacturer instructions (18). The KLM1 pancreatic cell line was provided by Dr. U. Rudloff (NCI, Bethesda, MD) in September 2011, The L55 lung adenocarcinoma cell line was provided by Dr. S. Albelda (University of Pennsylvania, PA). The MKN74 stomach cell line was provided by Dr. T. Yamori (Pharmaceuticals and Medical Device Agency, Japan), the HAY cells was provided by the Stehlin Foundation for Cancer Research (Houston, TX). The A431/H9 was transfected in our lab and previously described (19). Identity of all cell lines was confirmed by short tandem repeat (STR) testing within the past 12 months and all cell lines were tested negative for mycoplasma. A431/H9 cells were plated at 2.5×10^3 cells/well and other cell lines at 5×10^3 cells/well. All assays were run with four replicas and IC_{50}s calculated. All assays were repeated three times.

Cytotoxicity of RIT against early passage mesothelioma cell lines—Patient derived mesothelioma cells were isolated from the ascites or pleural fluid of four patients and frozen. Cell collection was approved in Clinical Protocols 08-C-0026 and 13-C-0202 by the Institutional Review Board of the National Cancer Institute. Cells were thawed and grown for 4 days and plated at 5×10^3 cells/well. Cell viability was determined using a WST8 cell-counting kit (Dojindo Molecular Technologies) (20, 21).

Collection of human PBMC

Apheresis samples were collected from volunteers under research protocols approved by the NIH Review Board (99-CC-0168). PBMC were isolated by gradient density separation using Ficoll-Hypaque (GE Healthcare, Piscataway, NJ) according to manufacturer's instructions. PBMC were viably frozen as previously described (22)

PBMC *in vitro* expansion—PBMC were thawed and plated in 6 well plates at 4×10^6 cells/ml. Cells were stimulated with either 5 μg/ml of SS1P or LMB-T20 for 4 days. On days 4, 8 and 11 half of the media was removed and replaced with media containing recombinant human IL-2 (500ng/ml) (Millipore IL002). On day 14, the cells were harvested, washed and restimulated. Cells that were expanded with SS1P were restimulated with 22 peptide pools spanning the sequence of WT PE38 as previously described (22). Cells that were expanded using LMB-T20 were restimulated with 15 peptide pools spanning the sequence of the deimmunized RIT. T cell activation was assessed using IL-2 ELISpot as described below. Once a pool had a positive response, the individual peptides in the pool were assessed with the same assay.

PBMC stimulation with whole protein—PBMC from 12 donors were plated at 2×10^6cells/well in pre-coated and pre-blocked ELISpot plates. Cells were stimulated with 50 μg/ml of SS1P, LMB-T20 or KLH (Fisher Scientific). Cells were placed at 37°C in a 5%

CO_2 incubator for 6 days. On day 7, plates were carefully removed from the incubator and cells were further treated with a second round of 50 μg/ml of the proteins. T cell activation was evaluated using IFNγ and IL-2 ELISpot. To lower endotoxin levels in the RITs, we used high capacity endotoxin removal spin columns (Thermo Fisher Scientific, Waltham, MA). SS1P and LMB-T20 used in these studies had <5EU/ml of endotoxin.

ELISpot—ELISpot antibodies were obtained from Mabtech, OH. Wells were coated with 1 μg of anti-human IL-2 (clone MT2A91/2C95) or anti-human IFNγ (clone 1-D1K) and incubated at 4°C for 18 hours. The following day, plates were washed 4 times with PBS and blocked using assay media (RPMI, 5% heat inactivated human AB serum (Gemini) and P/S antibiotic). After 30 minutes incubation at 37°C, plates were washed and human PBMC (1×10^5 cells/well) added. Cells were then stimulated with either peptides or whole protein and incubated for 18 hours. Next the plates were washed and secondary biotinylated anti-human IL-2 (clone MT8G10) or anti-IFNγ (clone 7-B6-1) was added and incubated at room temperature for 2 hours. The plates were then washed, streptavidin ALP (1:1000) added and incubated for 1 hour. Spots were detected using BCIP/NTB substrate solution (KPL, MD). Spots were counted by computer-assisted image analysis (Immunospot 5.0; Cellular Technology Limited).

Mouse xenograft tumor—Athymic nude mice were inoculated subcutaneously with 1×10^6 A431/H9 cells or 4×10^6 KLM1 cells with 4 mg/mL Matrigel (BD Biosciences). Intravenous treatment with LMB-T20 (5 mg/kg) or vehicle (PBS) began on day 7 when the tumors reached 100 mm^3. Mice were injected intravenously with RITs at the indicated amounts and indicated schedules, usually every day for a total of six doses. Body weight and tumor size were observed for 30 days. Mice were euthanized if they experienced rapid weight loss or a tumor burden greater than 10% body weight. No animals were excluded from statistical analysis. Tumor-sizes were measured using a caliper. Nonspecific toxicity was evaluated by intravenous (i.v.) injections of indicated doses in A431/H9 tumor bearing mice.

Mouse xenograft tumor with human patient's tumor cells—Cultured cells from patients NCI-Meso16 and NCI-Meso21 were injected in the flank of eight or 10 athymic nude mice as previously described (21). Cell collection was approved by Clinical Protocols 08-C-0026 and 13-C-0202 by the Institutional Review Board of the National Cancer Institute. Body weight and tumor size were evaluated twice a week. Once tumors reached an average of 100mm^3 (day 53 for NCI-Meso16 and day 88 for NCI-Meso21) LMB-T20 was injected intravenously according to the indicated schedules and dose. All mouse experiments followed NIH guidelines approved by the Animal Care and Use Committee of the NCI (ACUC).

Statistical analysis

Statistical analysis was conducted using Graphpad Prizm. Mann Whitney test was used to analyze the anti-tumor activity. For T cell activation assays and cytotoxicity assays, Freidman's test with Dunn's multiple comparison was used. Two way ANOVA was used to compare the epitope maps.

Results

Construction of RITs targeting mesothelin

SS1P is composed of an anti-mesothelin dsFv fused to a 38-kDa fragment of PE38 (Fig. 1A). PE38 is made up of two domains; domain II (amino acids 253–364) involved in toxin processing, and domain III (amino acids 395–613) contains the ADP ribosylation activity. We previously showed that modifying SS1P by deletion of the majority of domain II and retaining the 11 amino acid furin cleavage site followed by a GGS spacer results in a RIT (SS1-LR-GGS) (Fig. 1B) with high cytotoxic activity on many cell lines and much lower nonspecific toxicity in mice (18). To construct LMB-T20 we introduced six mutations (R427A, F443A, L477H, R494A, R505A and L552E) into SS1-LR-GGS (Fig. 1C and D). These mutations were previously shown to reduce T cell epitopes in an immunotoxin targeting CD22. Figure 1E shows an SDS gel that demonstrates the high purity of the RITs used in this study; SS1P has the expected size of 63-kDa, whereas SS1-LR-GGS and LMB-T20 have the expected size of 51-kDa.

T cell epitopes in LMB-T20 are diminished

To quantify the decrease in T cell epitope content and to determine if the changes in six amino acids that diminish the T cell epitope content could have affected the processing of the protein antigen (LMB-T20) or produced new T cell epitopes, we mapped the T cell epitopes in LMB-T20 and compared the results to the epitopes in SS1P. To do this we stimulated PBMC from 10 normal donors with SS1P or LMB-T20. After 14 days of *in vitro* expansion, the cells that were stimulated with SS1P were re-stimulated with 111 peptides spanning the sequence of PE38 and the cells that were stimulated with LMB-T20 were re-stimulated with 76 peptides spanning the entire sequence of LMB-T20. T cell activation was detected using IL-2 ELISpot (Fig. 2). To analyze the responses we divided the responses into nine categories based on the rate of response (as shown in the ladder in Figure 2 (on right) and the number of responses in each category.

We found that the PBMC samples stimulated with SS1P contained eight major epitopes as previously described (15). However, in cells that were stimulated with LMB-T20 there was an 81% reduction in the total response ($p>0.0001$ in 2-way ANOVA) from a total of 105 positive responses to SS1P to a total of 25 responses to LMB-T20. Also, peptides that did not induce responses after stimulation with SS1P also did not generate responses after stimulation with LMB-T20 (with the exception of three very minor responses), indicating that cryptic or new epitopes did not emerge as a result of altered antigen processing in LMB-T20.

Stimulation of PBMC with whole LMB-T20 protein

To evaluate the ability of LMB-T20 to induce a T cell response, we directly stimulated PBMC from 12 donors (with various DRB1 HLA haplotypes) with SS1P, LMB-T20 or KLH in ELISpot plates. After restimulation on day 7, plates were washed and detection IFNγ and IL-2 secreting cells was performed on day 8. PBMC stimulated with KLH had the strongest response with a median of 489 IL-2 Spot Forming Cells (SFC)/1×10^6 and 1951 IFNγ SFC/1×10^6 (Fig. 3A and 3B), which is consistent with the ability of KLH to stimulate

a strong T cell immune response (23). SS1P also produced a strong T cell response, which was significantly greater than the no protein control for both IFNγ and IL-2 ($p<0.0001$ and 0.001 respectively in Freidman test with Dunn's multiple comparisons) with a median of 702 IFNγ SFC/1×10^6 and 226 IL-2 SFC/1×10^6 in SS1P stimulated cells and a median of 10 IFNγ SFC/1×10^6 and 19 IL-2 SFC/1×10^6 in the no protein control. The PBMC response to LMB-T20 was very weak and not significantly stronger than that of the no protein control with a median of 163 SFC/1×10^6 and 91 SFC/1×10^6 for IFNγ and IL-2, respectively. Figure 3C shows examples of either IFNγ or IL-2 ELIspot wells of one of the PBMC samples that had a strong response to KLH and SS1P. In contrast, the cells stimulated with LMB-T20 had very few spots.

To our knowledge this is the first time the T cell immunogenicity of whole protein RITs have been evaluated and this assay can be used to evaluate T cell immunogenicity of future constructs.

Evaluation of activity of LMB-T20 in cancer cell lines

We next compared the activity of LMB-T20 with SS1-LR-GGS and with SS1P on five mesothelin expressing cancer cell lines from different types of cancer (Fig. 4 and Supplementary Table S1). These are mesothelioma, pancreatic, lung and stomach cancer and a mesothelin transfected epidermoid carcinoma (19). Mesothelin expression was previously evaluated by flow cytometry for all five cell lines and showed expression of more than 45,000 mesothelin per cell (3, 4, 19, 24). We found that LMB-T20 was very cytotoxic to all five cell lines and almost as active as SS1-LR-GGS that has no mutations in domain III. Both were much more cytotoxic than SS1P on cancer cell lines that express endogenous mesothelin.

Evaluation of cytotoxic activity on patients cells

Because SS1P has shown activity in some patients with mesothelioma (9, 25), we examined the activity of LMB-T20 on cells recently obtained from four mesothelioma patients. These cells more closely resemble cells growing in patients than established cell lines that have been propagated many years (20). These patient derived cells were previously shown to have high mesothelin expression (20, 21). We found that LMB-T20 was more active than SS1P in cytotoxicity assays on all four patient derived lines (Supplementary Fig. S1) with lower IC_{50} values (Fig. 5) in all four patient samples, and that it had similar activity to that of its parental RIT (SS1-LR-GGS).

Anti-tumor activity of deimmunized RITs in mouse xenograft model

To evaluate the efficacy of LMB-T20 *in vivo*, A431/H9 cells were inoculated into the flank of 16 athymic nude mice. On days 5, 6, 7, 8, 9 and 13 after injection, eight mice were treated intravenously with 5mg/kg of LMB-T20 (Fig. 6A) and another eight mice were treated with vehicle. On day 9, a significant decrease in tumor size was observed ($p<0.01$ in Mann Whitney test) and 2/8 mice had a complete response; the other five mice had complete responses by day 15 and complete responses persisted in 7/8 mice until day 60 when the experiment was terminated. LMB-T20 was well tolerated with no weight loss in the treated mice.

We evaluated the anti-tumor activity of LMB-T20 in a pancreatic tumor model, by inoculating mice with KLM1 cells. The mice were treated with intravenous LMB-T20 at the same dose as the A431/H9 xenograft model on days 7, 8, 9, 10, 12, 13 (Fig. 6B). We observed a significant delay in tumor growth starting on day 9 ($p<0.05$ in Mann Whitney test) in the mice treated with LMB-T20. A significant growth delay of 11 days was observed ($p=0.008$ in the Wilcoxon matched rank test).

Anti-tumor activity of LMB-T20 against patients cells grown *in vivo*

To evaluate the activity of LMB-T20 in tumors derived from early passage mesothelioma tumor cells (21), cells from patient NCI-Meso16 were inoculated into eight athymic mice and cells from patient NCI-Meso21 inoculated in 10 additional mice. These tumors, like tumors in mesothelioma patients, grew more slowly than our A431/H9 model and it took 53 days to reach an average size of $107mm^3$ (Fig. 6C). Mice were then treated intravenously with 5mg/kg of LMB-T20 daily or with vehicle and tumor size measured every other day. On day 55, a significant difference between the treatment groups was observed ($p<0.03$ Mann Whitney test), with an average tumor size of $110mm^3$ for tumors treated with LMB-T20 and $168mm^3$ for tumors treated with vehicle. This growth delay lasted until day 65 when the tumors started to regrow.

Mice that were inoculated with patients cells NCI-Meso21 had a better anti-tumor response compared to NCI-Meso16. Tumors in these mice grew more slowly and reached $102mm^3$ on day 88 (Fig. 6D). Mice were treated daily starting day 88 intravenously with 5mg/kg of LMB-T20 or vehicle and a significant decrease in tumor size was observed as early as day 90, in which the average tumor size in LMB-T20 treated mice was $87mm^3$ while the vehicle treated tumors grew to $120mm^3$ ($p<0.008$ Mann Whitney test). By day 104, tumor growth of both treatment groups was arrested.

Mouse toxicity

To further assess the non-specific toxicity of LMB-T20 and SS1-LR-GGS in mice, we treated small groups of tumor bearing nude mice with increasing doses of RIT (Supplementary Table S2). In the anti-tumor experiments shown in Figure 6, a dose of 5mg/kg every day for 6 days was well tolerated with no weight loss or other toxicities. In the current study we observed that two doses of 15mg/kg of LMB-T20 produced a 9% weight loss and that a higher dose of 20mg/kg caused the death of 1/2 mice. LR-GGS was more toxic than LMB-T20; 2/2 mice treated with 10mg/kg had severe weight loss and had to be euthanized.

Discussion

We describe here the properties of LMB-T20, a new RIT designed to target cancers expressing mesothelin. T cell activation assays show that LMB-T20 has greatly decreased immunogenicity compared with its parent SS1P that contains a 38-kDa form of the toxin. Despite this very large decrease in immunogenicity, LMB-T20 is significantly more active than SS1P in killing mesothelin expressing cancer cell lines and in inducing regressions of mesothelin-expressing tumors in mice. To determine if the immunogenicity of the mutant

toxin was diminished, we re-mapped the epitopes in the de-immunized toxin and found they were significantly reduced. We were also concerned that the six amino acid mutations introduced into the toxin might alter processing and unveil cryptic or subdominant epitopes as reported by Liu *et al*. (26), but we did not observe this in our study.

The toxin in LMB-T20 is similar to one recently reported in an immunotoxin targeting CD22 expressing cells (15). In those studies the cytotoxic activity of the de-immunized immunotoxin was similar to that of the parental immunotoxin containing PE38. In the current study, using the same mutant toxin, we find that the new anti-mesothelin immunotoxin is 2–3 fold more active than SS1P on cancer cell lines. It is 3–20 fold more active than SS1P in killing mesothelioma cells recently obtained from patients, which have not undergone changes that allow continuous growth in culture. The reason for the increase in activity has not been determined; we suggest that it is likely due to more efficient intracellular trafficking from the cell surface to the cytosol where the toxin ADP-ribosylates EF2.

We also assessed the activity of LMB-T20 in four mouse tumor models. Using the A431/H9 tumor model, we observed a complete response in 7/8 of the tumors. Using the pancreatic cancer KLM1 model we observed stabilization of tumor growth. We also examined the effect of LMB-T20 on slow growing tumors resulting from injection of mesothelin expressing cells recently obtained from patients into mice and observed a decrease in tumor size in one tumor and stabilization of the second. Pancreatic cancer and mesothelioma are notoriously resistant to most chemotherapeutic agents. Therefore, it is not surprising that a monotherapy cannot eradicate such tumors. We have previously reported strong synergy when immunotoxins targeting mesothelin are combined with Taxanes (3). We have not yet carried out such studies with the mutant immunotoxins and plan to do so.

It would be very useful to be able to determine the immunogenicity of new mutant proteins directly without having to synthesize new mutant peptides for each mutation introduced. For example LMB-T20 has six amino acid mutations in domain III. Determination of immunogenicity of different protein candidates was previously performed by pulsing dendritic cells with the whole proteins followed by addition of autologous T cells, whose activation was detected using T cell proliferation or cytokine secretion (27, 28). Here, we used a simplified approach and eliminated the dendritic cell maturation step, because we found that components in the PBMC can process enough antigen to present the T cells (22, 29). We chose to evaluate both IFNγ and IL-2 cytokines because they complement each other for a more comprehensive coverage of the entire helper T cell response in that IFNγ is active in Th1 polarization and IL-2 in Th2 cells (30). We also chose to evaluate the median and not mean of the 12 donor responses, because the median is less sensitive to outliers and to donor-to-donor variations we observed in this assay.

Conclusion

In this work we describe the development and characterization of a highly potent de-immunized RIT that can be used for multiple types of cancers that express mesothelin. It promotes partial and complete responses in mice xenograft models and can be given in

higher and more frequent doses due to its reduced non-specific toxicity. Because of its low immunogenicity and high cytotoxic and anti-tumor activity, we believe LMB-T20 warrants further pre-clinical development.

Supplementary Material

Refer to Web version on PubMed Central for supplementary material.

Acknowledgments

Funding: This research was supported by the Intramural Research Program of the NIH, National Cancer Institute, Center for Cancer Research and with a Cooperative Research and Development Agreement (#2791) with Roche Pharmaceuticals.

Abbreviation List

ADA	anti-drug antibodies
IFNβ	interferon beta
PE38	*Pseudomonas* exotoxin
RITs	recombinant immunotoxins
V_H	heavy-chain Fv
V_L	light-chain Fv

References

1. Kreitman RJ, Tallman MS, Robak T, Coutre S, Wilson WH, Stetler-Stevenson M, et al. Phase I trial of anti-CD22 recombinant immunotoxin moxetumomab pasudotox (CAT-8015 or HA22) in patients with hairy cell leukemia. J Clin Oncol. 2012; 30:1822–8. [PubMed: 22355053]
2. Kreitman RJ, Wilson WH, White JD, Stetler-Stevenson M, Jaffe ES, Giardina S, et al. Phase I trial of recombinant immunotoxin anti-Tac(Fv)-PE38 (LMB-2) in patients with hematologic malignancies. J Clin Oncol. 2000; 18:1622–36. [PubMed: 10764422]
3. Hollevoet K, Mason-Osann E, Liu XF, Imhof-Jung S, Niederfellner G, Pastan I. In vitro and in vivo activity of the low-immunogenic antimesothelin immunotoxin RG7787 in pancreatic cancer. Mol Cancer Ther. 2014; 13:2040–9. [PubMed: 24928849]
4. Alewine C, Xiang L, Yamori T, Niederfellner G, Bosslet K, Pastan I. Efficacy of RG7787, a next-generation mesothelin-targeted immunotoxin, against triple-negative breast and gastric cancers. Mol Cancer Ther. 2014; 13:2653–61. [PubMed: 25239937]
5. Hassan R, Kreitman RJ, Pastan I, Willingham MC. Localization of mesothelin in epithelial ovarian cancer. Appl Immunohistochem Mol Morphol. 2005; 13:243–7. [PubMed: 16082249]
6. Tang Z, Qian M, Ho M. The role of mesothelin in tumor progression and targeted therapy. Anticancer Agents Med Chem. 2013; 13:276–80. [PubMed: 22721387]
7. Kreitman RJ, Hassan R, Fitzgerald DJ, Pastan I. Phase I trial of continuous infusion anti-mesothelin recombinant immunotoxin SS1P. Clin Cancer Res. 2009; 15:5274–9. [PubMed: 19671873]
8. Hassan R, Bullock S, Premkumar A, Kreitman RJ, Kindler H, Willingham MC, et al. Phase I study of SS1P, a recombinant anti-mesothelin immunotoxin given as a bolus I.V. infusion to patients with mesothelin-expressing mesothelioma, ovarian, and pancreatic cancers. Clin Cancer Res. 2007; 13:5144–9. [PubMed: 17785569]
9. Hassan R, Miller AC, Sharon E, Thomas A, Reynolds JC, Ling A, et al. Major cancer regressions in mesothelioma after treatment with an anti-mesothelin immunotoxin and immune suppression. Sci Transl Med. 2013; 5:208ra147.

10. Schellekens H. How to predict and prevent the immunogenicity of therapeutic proteins. Biotechnol Annu Rev. 2008; 14:191–202. [PubMed: 18606364]
11. Malucchi S, Sala A, Gilli F, Bottero R, Di Sapio A, Capobianco M, et al. Neutralizing antibodies reduce the efficacy of betaIFN during treatment of multiple sclerosis. Neurology. 2004; 62:2031–7. [PubMed: 15184610]
12. Baert F, Noman M, Vermeire S, Van Assche G, GDH, Carbonez A, et al. Influence of immunogenicity on the long-term efficacy of infliximab in Crohn's disease. N Engl J Med. 2003; 348:601–8. [PubMed: 12584368]
13. Onda M, Beers R, Xiang L, Nagata S, Wang QC, Pastan I. An immunotoxin with greatly reduced immunogenicity by identification and removal of B cell epitopes. Proc Natl Acad Sci USA. 2008; 105:11311–6. [PubMed: 18678888]
14. Yeung VP, Chang J, Miller J, Barnett C, Stickler M, Harding FA. Elimination of an immunodominant CD4+ T cell epitope in human IFN-beta does not result in an in vivo response directed at the subdominant epitope. J Immunol. 2004; 172:6658–65. [PubMed: 15153481]
15. Mazor R, Eberle JA, Hu X, Vassall AN, Onda M, Beers R, et al. Recombinant immunotoxin for cancer treatment with low immunogenicity by identification and silencing of human T-cell epitopes. Proc Natl Acad Sci USA. 2014; 111:8571–6. [PubMed: 24799704]
16. Chowdhury PS, Viner JL, Beers R, Pastan I. Isolation of a high-affinity stable single-chain Fv specific for mesothelin from DNA-immunized mice by phage display and construction of a recombinant immunotoxin with anti-tumor activity. Proc Natl Acad Sci USA. 1998; 95:669–74. [PubMed: 9435250]
17. Pastan I, Beers R, Bera TK. Recombinant immunotoxins in the treatment of cancer. Methods Mol Biol. 2004; 248:503–18. [PubMed: 14970517]
18. Weldon JE, Xiang L, Chertov O, Margulies I, Kreitman RJ, FitzGerald DJ, et al. A protease-resistant immunotoxin against CD22 with greatly increased activity against CLL and diminished animal toxicity. Blood. 2009; 113:3792–800. [PubMed: 18988862]
19. Ho M, Hassan R, Zhang J, Wang QC, Onda M, Bera T, et al. Humoral immune response to mesothelin in mesothelioma and ovarian cancer patients. Clin Cancer Res. 2005; 11:3814–20. [PubMed: 15897581]
20. Zhang J, Qiu S, Zhang Y, Merino M, Fetsch P, Avital I, et al. Loss of mesothelin expression by mesothelioma cells grown in vitro determines sensitivity to anti-mesothelin immunotoxin SS1P. Anticancer Res. 2012; 32:5151–8. [PubMed: 23225411]
21. Kalra N, Zhang J, Thomas A, Xi L, Cheung M, Talarchek J, et al. Mesothelioma patient derived tumor xenografts with defined BAP1 mutations that mimic the molecular characteristics of human malignant mesothelioma. BMC Cancer. 2015; 15:376. [PubMed: 25952750]
22. Mazor R, Vassall AN, Eberle JA, Beers R, Weldon JE, Venzon DJ, et al. Identification and elimination of an immunodominant T-cell epitope in recombinant immunotoxins based on Pseudomonas exotoxin A. Proc Natl Acad Sci USA. 2012; 109:E3597–603. [PubMed: 23213206]
23. Musselli C, Livingston PO, Ragupathi G. Keyhole limpet hemocyanin conjugate vaccines against cancer: the Memorial Sloan Kettering experience. J Cancer Res Clin Oncol. 2001; 127 (Suppl 2):R20–6. [PubMed: 11768620]
24. Tang Z, Feng M, Gao W, Phung Y, Chen W, Chaudhary A, et al. A human single-domain antibody elicits potent antitumor activity by targeting an epitope in mesothelin close to the cancer cell surface. Mol Cancer Ther. 2013; 12:416–26. [PubMed: 23371858]
25. Pastan I, Hassan R. Discovery of mesothelin and exploiting it as a target for immunotherapy. Cancer Res. 2014; 74:2907–12. [PubMed: 24824231]
26. Liu Z, Williams KP, Chang YH, Smith JA. Immunodominance: a single amino acid substitution within an antigenic site alters intramolecular selection of T cell determinants. J Immunol. 1993; 151:1852–8. [PubMed: 7688387]
27. Schlienger K, Craighead N, Lee KP, Levine BL, June CH. Efficient priming of protein antigen-specific human CD4(+) T cells by monocyte-derived dendritic cells. Blood. 2000; 96:3490–8. [PubMed: 11071646]
28. Jaber A, Baker M. Assessment of the immunogenicity of different interferon beta-1a formulations using ex vivo T-cell assays. J Pharm Biomed Anal. 2007; 43:1256–61. [PubMed: 17118612]

29. Oseroff C, Sidney J, Kotturi MF, Kolla R, Alam R, Broide DH, et al. Molecular determinants of T cell epitope recognition to the common Timothy grass allergen. J Immunol. 2010; 185:943–55. [PubMed: 20554959]

30. Zhang Y, Zhang Y, Gu W, Sun B. TH1/TH2 cell differentiation and molecular signals. Adv Exp Med Biol. 2014; 841:15–44. [PubMed: 25261203]

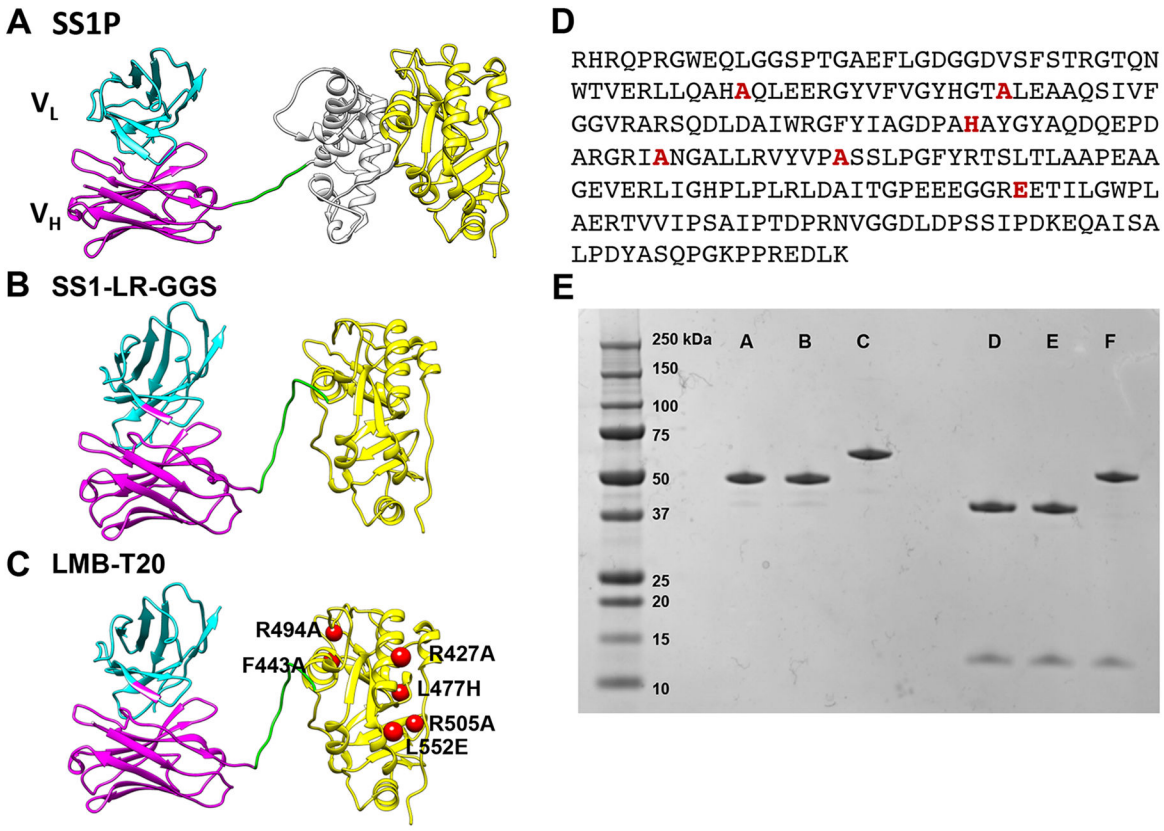

Figure 1.

Structural models of RITs. SS1P consists of a disulfide-stabilized heavy chain Fv polypeptide (V_H) (cyan) and light chain Fv polypeptide (V_L) (magenta) that are coupled to a 38-kDa fragment of PE38. **(A)** V_H is recombinantly conjugated to the toxin fragment, which is composed of domain II (gray) and domain III (yellow). **(B)** SS1-LR-GGS. The SS1 Fv is conjugated to domain III with GGS linker between the furin cleavage site and domain III. **(C)** LMB-T20. Six point mutations were introduced into the scaffold of SS1-LR-GGS to diminish T cell epitopes. (**D**) Amino acid sequence of the toxin in LMB-T20. (**E**) SDS gel (4–20%) run under non-reducing conditions (lanes A, B and C) and reducing conditions (D, E and F) show the size and purity of the variant immunotoxins. Lanes A and D, LMB-T20, lanes B and E, LR-GGS and lanes C and F, SS1P.

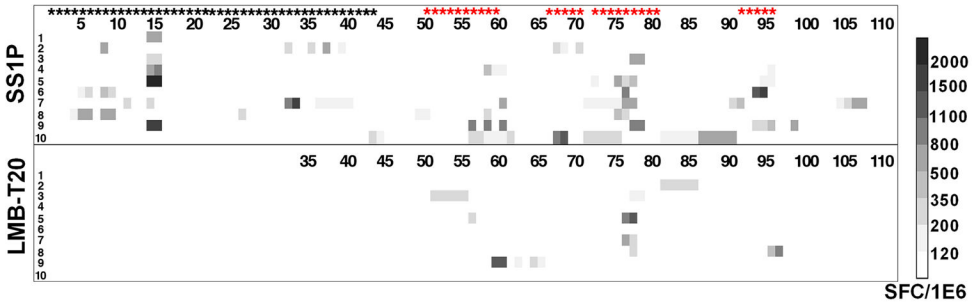

Figure 2.

Stimulation of PBMC from 10 donors with LMB-T20 and SS1P show a decrease in T cell activation. PBMC from 10 naïve donors were stimulated with either SS1P or LMB-T20. After 14 days of *in vitro* expansion cells that were re-stimulated with either 111 peptides spanning the sequence of PE38 or 76 peptides spanning the sequence of LMB-T20. T cell activation was detected using IL-2 ELISpot. All positive peptides were assayed twice for each PBMC sample and each assay was run in triplicate. Response strength is shown in the SFC ladder on the right. Black stars represent peptides that were deleted in LMB-T20 and red stars represent peptides that are different from wild type.

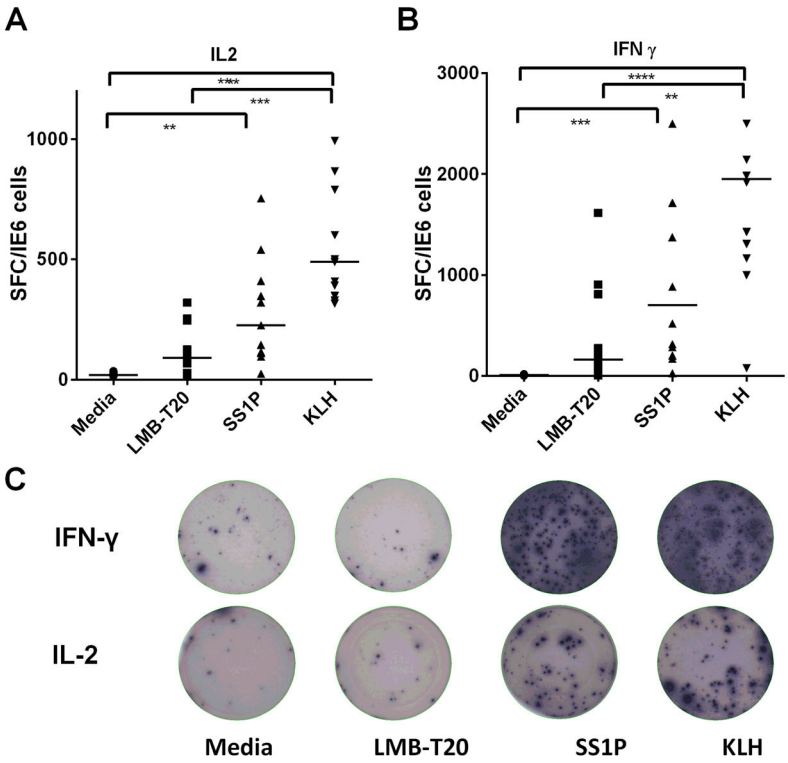

Figure 3.

Stimulation of human PBMC with LMB-T20 results in a significantly diminished T cell epitopes. PBMC from 10 donors were plated in pre-coated blocked ELISpot plates and stimulated with 50 μg/ml of LMB-T20, SS1P or KLH or nothing diluted in media. After 6 days cells were treated with a second boost of 50 μg/ml of the respective proteins. T cell activation was evaluated using IFNγ and IL-2 ELISpot. **A.** IL-2 response. **B.** IFNγ response. Lines represent medians. **** $p<0.0001$ ***$p<0.001$ and **$p<0.01$ in Freidman test with Dunn's multiple comparisons. **C**. Representative ELISpot wells after spot detection. All donors and stimulations were run in four replicas and the assay was repeated for 10 of the 12 samples. The other two samples were not repeated because the PBMC samples were not abundant enough for two experiments. One sample was invalidated because the response did not repeat in the second IL-2 assay.

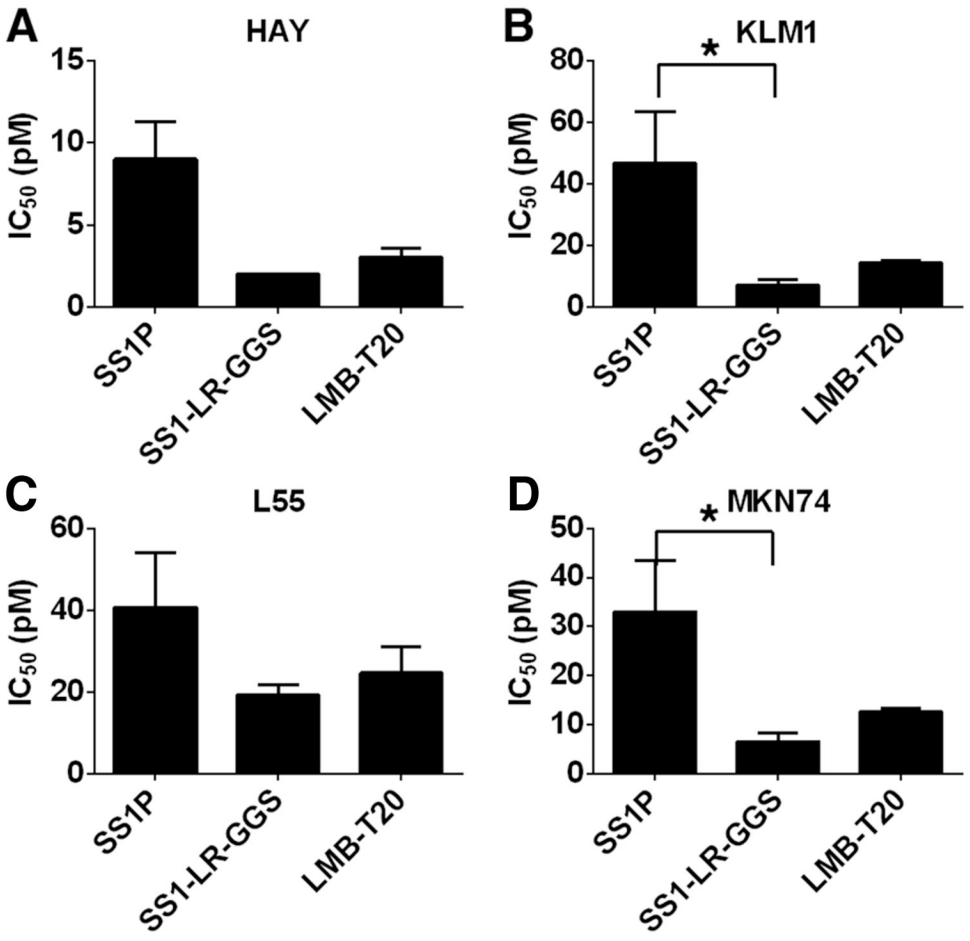

Figure 4.

Cytotoxic activity of LMB-T20 on cells that express endogenous mesothelin. The cytotoxicity of LMB-T20 with SS1P and LR-GGS was compared in a panel of four cell lines; (A) HAY, (B) KLM1 (C) L55 and (D) MKN74. For each cell line, the mean IC_{50} of three assays is shown. Summary of all IC_{50}s for all cell lines is shown in Supplementary Table S1. Error bars represents SEM. *$p<0.05$ in Freidman test with Dunn's multiple comparisons.

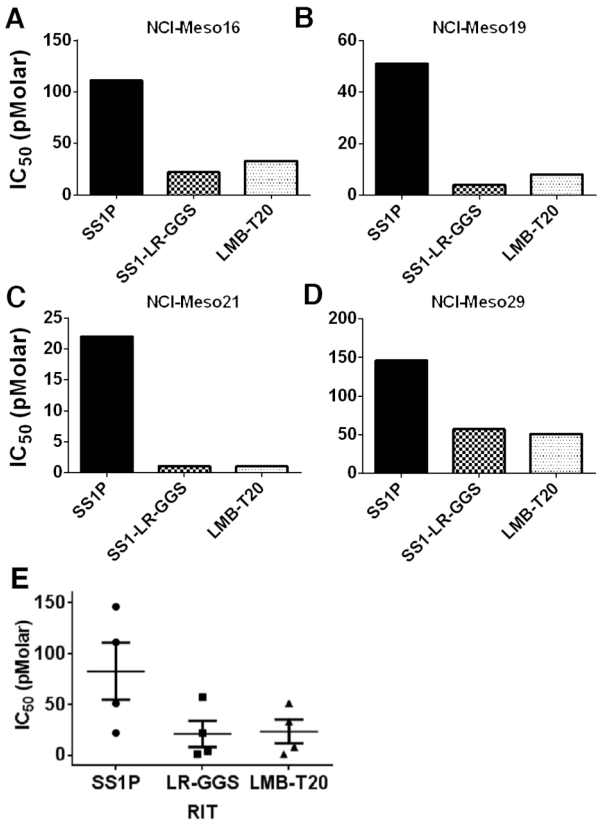

Figure 5.

Activity of mesothelin targeting RITs on mesothelioma patient cells. Cells cultured from the pleural fluid or ascites of four mesothelioma patients **(A)** NCI-Meso16, **(B)** NCI-Meso19, **(C)** NCI-Meso21, and **(D)** NCI-Meso29) were treated with increasing concentrations of RITs. After 72 hours, cells were evaluated for viability using a WST-8 assay and IC_{50} were calculated. **(E)** Mean of IC_{50} for the four samples. Cells were treated in three replicas. Line represents mean, error bar show SEM

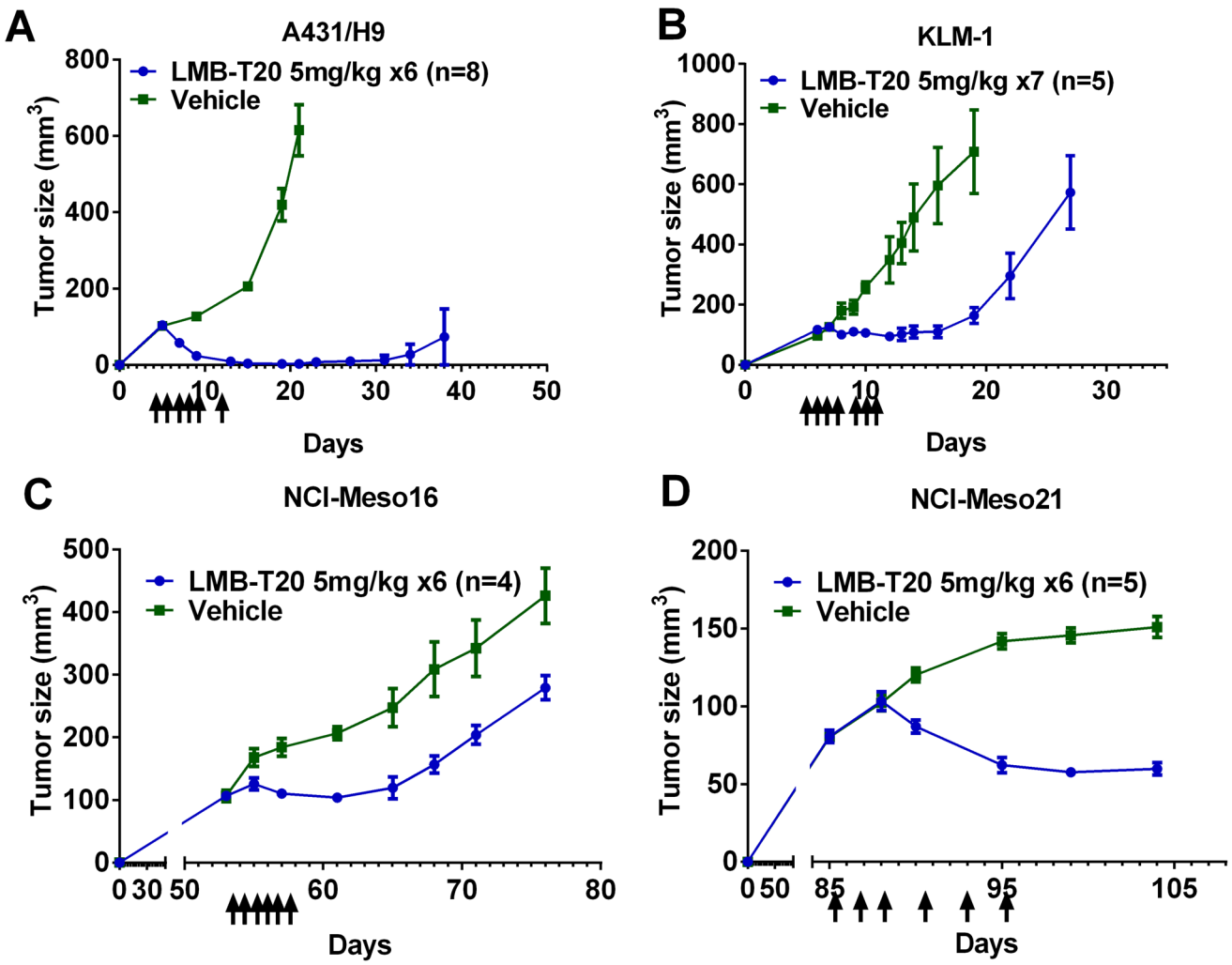

Figure 6.

Effect of deimmunized RITs on mouse xenograft tumor model. Arrows indicate the days that treatment was administered. **(A)** Female athymic nude mice were inoculated with 10^6 A431/H9 cells at time 0. Intravenous treatment with LMB-T20 (5mg/kg) or vehicle began on day 5 and continued every day for a total of six doses. Average of mean tumor volume for *n* = 8 animals treated with LMB-T20 or vehicle. On day 38 one of the mice in LMB-T20 group was euthanized due to tumor burden and thus averages after this time point cannot be shown. A significant decrease in tumor size was observed on day 9 ($p<0.01$ in Mann Whitney test) and every measurement after that time point until day 38. **(B)** Female athymic nude mice were inoculated with 4×10^6 KLM1 cells at time 0. Intravenous treatment with LMB-T20 (5mg/kg) or vehicle began on day 7 and continued every day for a total of seven doses. Each data point represents average of mean tumor volume for *n* = 5 animals treated with LMB-T20 or vehicle. Significant differences between tumor size was observed between the two treatment groups starting on day 9 ($p<0.05$ in Mann Whitney test). On day 29 the experiment was terminated when all mice in the treated group had tumors >500mm^3. **(C)** Female SCID mice were injected with cells obtained from ascitic fluids of patient NCI-M-16. On day 53, when tumor reached 100mm^3, six doses of 5mg/kg LMB-T20 were

injected intravenously every day. A significant difference in tumor size was observed beginning on day 55 ($P<0.03$) in Mann Whitney test. **(D)** Ten SCID mice were injected with cells obtained from ascites of patient NCI-M-21. On day 88, six doses of 5mg/kg LMB-T20 were injected intravenously every other day. A significant difference in tumor size was observed beginning on day 90 ($P<0.007$) in Mann Whitney test. Error bars indicate SEM.